Targeted Chromosomal Translocations and Essential Gene Knockout Using CRISPR/Cas9 Technology in *Caenorhabditis elegans*

Xiangyang Chen,[1] Mu Li,[1] Xuezhu Feng,[2] and Shouhong Guang[2]
School of Life Sciences, University of Science and Technology of China, Hefei, Anhui 230027, People's Republic of China

ABSTRACT Many genes play essential roles in development and fertility; their disruption leads to growth arrest or sterility. Genetic balancers have been widely used to study essential genes in many organisms. However, it is technically challenging and laborious to generate and maintain the loss-of-function mutations of essential genes. The CRISPR/Cas9 technology has been successfully applied for gene editing and chromosome engineering. Here, we have developed a method to induce chromosomal translocations and produce genetic balancers using the CRISPR/Cas9 technology and have applied this approach to edit essential genes in *Caenorhabditis elegans*. The co-injection of dual small guide RNA targeting genes on different chromosomes resulted in reciprocal translocation between non-homologous chromosomes. These animals with chromosomal translocations were subsequently crossed with animals that contain normal sets of chromosomes. The F1 progeny were subjected to a second round of Cas9-mediated gene editing. Through this method, we successfully produced nematode strains with specified chromosomal translocations and generated a number of loss-of-function alleles of two essential genes (*csr-1* and *mes-6*). Therefore, our method provides an easy and efficient approach to generate and maintain loss-of-function alleles of essential genes with detailed genetic background information.

KEYWORDS CRISPR/Cas9; chromosomal translocation; essential gene knockout; balancer

ESSENTIAL genes are required for the development and fertility of organisms. Loss-of-function mutations of essential genes usually result in growth arrest or sterility. The production and maintenance of homozygous mutants of the essential genes are demanding and time-consuming. A series of strains with particular chromosomal rearrangements, such as duplications, translocations, and inversions, have been generated and applied to screen and grow lethal or sterile mutants. Conventional methods to elicit chromosomal rearrangements involved treating the animals with ion irradiation or chemical mutagens (Jones *et al.* 2011). However, the majority of existing balancer strains lack detailed sequence information. Additionally, many unintended mutations are introduced during mutagenesis and are difficult to eliminate by backcrossing with wild-type strains. Therefore, it is critical to develop a more efficient method to produce balancer strains with detailed sequence information and nominal background mutations. Furthermore, the development of more effective approaches to generate and maintain loss-of-function mutations of particular essential genes is required.

Recent research in targeted genome editing has made inspiring progress in genome engineering, among which is the clustered regularly interspaced short palindromic repeats (CRISPR) technology (Cong *et al.* 2013; Jiang *et al.* 2013; Mali *et al.* 2013; Ran *et al.* 2013; Wang *et al.* 2013; Hsu *et al.* 2014; Shalem *et al.* 2014; Sternberg *et al.* 2014; Wang *et al.* 2014). In the CRISPR/Cas9 system, small guide RNA (sgRNA) targets its complementary genomic DNA and subsequently recruits the Cas9 nuclease to generate double-stranded DNA breaks (DSBs). As a consequence of nonhomologous end joining (NHEJ) repair, mutations are incorporated at the targeted sites.

In addition to editing a single gene, the CRISPR/Cas9 technology has also been applied to elicit chromosomal rearrangements in mammalian cell lines (Piganeau *et al.* 2013;

doi: 10.1534/genetics.115.181883
Manuscript received August 11, 2015; accepted for publication October 9, 2015; published Early Online October 16, 2015.
Supporting information is available online at www.genetics.org/lookup/suppl/doi:10.1534/genetics.115.181883/-/DC1.
[1]These authors contributed equally to this work.
[2]Corresponding authors: University of Science and Technology of China, School of Life Sciences, Huangshan Road 443, Hefei, Anhui 230027, People's Republic of China. E-mail: sguang@ustc.edu.cn; University of Science and Technology of China, School of Life Sciences, Huangshan Road 443, Hefei, Anhui 230027, People's Republic of China. E-mail: fengxz@ustc.edu.cn

Choi and Meyerson 2014; Ghezraoui *et al.* 2014; Torres *et al.* 2014; Kannan *et al.* 2015). A number of double-stranded DNA breaks can be induced in the presence of multiple guide RNAs. Thereafter, large genomic fragments can be reversed, deleted, or translocated to other chromosomal loci. These induced chromosomal rearrangements have been used to study the mechanism underlying cancers elicited by chromosomal inversions or translocations.

The CRISPR/Cas9 technology has been successfully applied to directing gene editing in *Caenorhabditis elegans* (Chen *et al.* 2013; Chiu *et al.* 2013; Cho *et al.* 2013; Dickinson *et al.* 2013; Friedland *et al.* 2013; Frokjaer-Jensen 2013; Katic and Grosshans 2013; Lo *et al.* 2013; Waaijers *et al.* 2013; Arribere *et al.* 2014; Chen *et al.* 2014; Kim *et al.* 2014; Paix *et al.* 2014; Farboud and Meyer 2015; Li *et al.* 2015; Ward 2015). However, there are no reports concerning Cas9-mediated genome rearrangements in *C. elegans*. Our previous work showed that large chromosome fragments of up to 24 kb can be eliminated through the co-injection of two sgRNAs in *C. elegans* (Chen *et al.* 2014). Here, we report the use of dual sgRNA-guided Cas9 nuclease to direct reciprocal chromosomal translocations in *C. elegans*. We developed a method to generate and maintain alleles of essential genes. Through the combination of chromosomal translocation strains and the CRISPR/Cas9 technology, the loss-of-function mutations of essential genes can be rapidly generated, and the mutants can be easily maintained through the balancer system, thereby providing an effective approach to study these genes.

Materials and Methods

Strains

Bristol strain N2 was used as the standard wild-type strain. All strains were incubated on nematode growth medium (NGM) plates seeded with OP50 at 20° (Brenner 1974). The following strains were used: GR1373—*eri-1(mg366)*, RB1441—*tag-349(ok1664)*, YY166—*ergo-1(gg98)*, RB1870—*clec-49(ok2416)*, VC2575—*y75b8a.11(ok3346)*, SHG373—*dpy-13(ust40)*, SHG376—*rde-12(ust17)*, and CB845—*unc-30(e191)*.

Construction of sgRNA expression plasmids

We manually searched for target sequences consisting of G $(N)_{19}$NGG near the desired mutation sites (Friedland *et al.* 2013). The target sequences are listed in Supporting Information, Table S1. We replaced the *unc-119* target sequence in the pU6::unc-119 sgRNA expression vector (Friedland *et al.* 2013) with the desired target sequence using overlap extension PCR. The pU6::unc-119 sgRNA vector was diluted to 2 ng/μl and PCR-amplified to generate linear products. The PCR products were digested by the *Dpn*I restriction enzyme and transformed into Trans10 Chemically Competent Cells (Transgene Biotech, Beijing). We used the Phanta Super-Fidelity DNA polymerase (Vazyme Biotech, Nanjing, China, catalog no. P501-d1/d2/d3) in all PCR reactions. The primer sequences used for the construction of the sgRNA expression plasmids are listed in Table S2.

Imaging

Images were collected using Leica DM2500 and M165 FC microscopes.

Microinjection

Cas9-mediated chromosomal translocations: DNA mixtures were microinjected into the gonads of young adult *C. elegans*. For the chromosomal translocation experiments, we injected 50 ng/μl of the Cas9 expression vector, 50 ng/μl of the sgRNA #1 and 50 ng/μl of the sgRNA #2 expression vectors (as indicated in the figures), and 5 ng/μl of the pCFJ90 vector (a co-injection marker that expressed mCherry fluorescent protein in the pharynx). After recovering from the injection, four to five worms were placed onto individual NGM plates. Three days after the injection, F1 animals expressing mCherry were transferred to individual NGM plates and allowed to produce F2 progeny for 2–3 days. From an F2 plate with both wild-type and dumpy morphology animals, six to eight dumpy animals were transferred to a new NGM plate to lay F3 progeny. For an F2 plate with 100% dumpy animals, no transfer was required. Then, F2 and F3 animals were harvested and washed in M9 buffer, transferred to 50 μl lysis buffer (500 μg/ml Proteinase K, 100 mM NaCl, 50 mM Tris, and 20 mM EDTA), and screened by PCR with primers outside of the sgRNA-targeted regions. The primer sequences used for PCR screening are listed in Table S3. Mutants with chromosomal translocations were singly transferred to NGM plates and verified by PCR amplification and DNA sequencing.

Construction of balancer strains and knockout of essential genes using the CRISPR/Cas9 technology (see Figure 4 for detailed illustration): Ten males of the chromosomal translocation strain *ustT2[ben-1;dpy-13](III,IV)* were mated with five hermaphrodites of CB845:*unc-30(e191)* at 15°. The *ustT2[ben-1;dpy-13](III,IV)* strain possesses the chromosomal translocation between LG III and LG IV that disrupts both *ben-1* and *dpy-13*. Both *dpy-13* and *unc-30* were used as visible markers to facilitate mutant screening and maintenance. Two days later, the hermaphrodites were singly transferred to individual NGM plates to lay F1 progeny. F1 animals with wild-type morphology were selected for microinjection. We injected 50 ng/μl of the Cas9 expression plasmid, 50 ng/μl of the sgRNA #1, 50 ng/μl of the sgRNA #2, and 50 ng/μl of the sgRNA #3 expression plasmids (as indicated in the figures), and 5 ng/μl of the pSG259 (Pmyo-2::GFP::unc-54utr) plasmid. After recovering from the injection, four to five injected worms were placed onto individual NGM plates. The F1 animals produced F2 progeny with different morphological phenotypes: uncoordinated (Unc), dumpy (Dpy), and wild type. Three days after the injection, F2 animals with wild-type morphology and GFP expression in the pharynx were singly transferred to individual NGM plates and allowed to produce F3 progeny for 2–3 days. By analyzing the linkage between lethality and the dumpy (Dpy) or uncoordinated (Unc) phenotype, the alleles of essential *gene X* can be identified. Meanwhile, all the F2 animals were transferred to 20 μl lysis

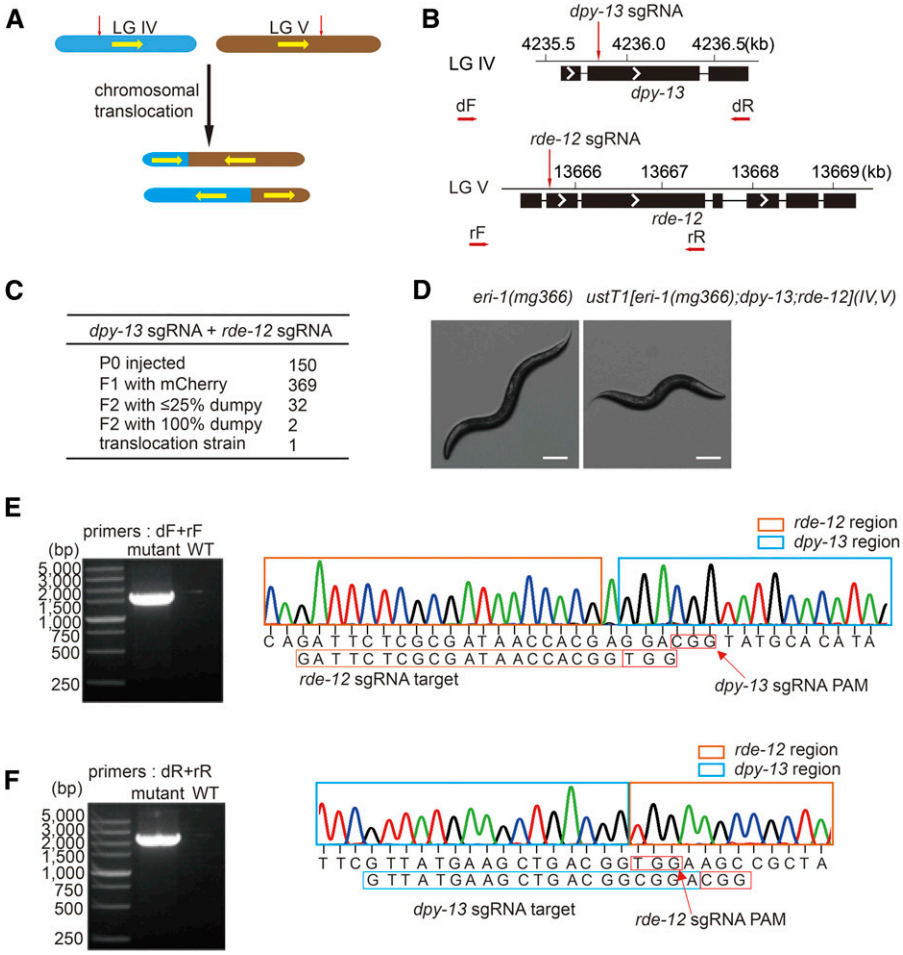

Figure 1 Cas9 directs chromosomal translocation between *dpy-13 (LG IV)* and *rde-12 (LG V)*. (A) Schematic depicting the overall strategy of generating chromosomal rearrangements. The red arrows indicate the sgRNA targets, and the yellow arrows show the orientation of chromosomes. (B) Schematic of the *rde-12* and *dpy-13* genes. Positions of sgRNA-guided cleavage sites and PCR primers for genotyping are indicated. (C) Summary of the microinjection experiments. (D) The chromosomal translocation strain *ustT1[eri-1(mg366);dpy-13;rde-12](IV,V)* exhibited a dumpy phenotype. (E and F) PCR amplification (left) and chromatogram of DNA sequencing (right) of the *ustT1[eri-1(mg366); dpy-13](IV)* and *ustT1[rde-12](V)* chromosomes. Breakpoints and sgRNA targets are indicated. Bars, 100 μm.

buffer and subjected to single-worm PCR to directly screen for mutants with large chromosomal deletions.

For the *csr-1* knockout experiment, the F3 plates were examined for the linkage between sterility and morphological markers. Then, six to eight dumpy sterile F3 animals or six to eight uncoordinated sterile F3 animals were transferred to 30 μl lysis buffer and verified by PCR and DNA sequencing.

For the *mes-6* knockout experiment, six to eight F3 dumpy young adults or six to eight F3 uncoordinated young adults were transferred to individual plates to produce F4 progeny and used to assess the linkage between the sterility phenotype and morphological markers. Then, six to eight dumpy sterile F4 animals or six to eight uncoordinated sterile F4 animals were transferred to 30 μl lysis buffer and verified by PCR amplification and DNA sequencing. For plates in which all F3 animals were sterile, four to five F3 dumpy worms and four to five F3 uncoordinated animals were transferred to 30 μl of lysis buffer and examined by PCR amplification and DNA sequencing. The primer sequences used for genotyping are listed in Table S4.

RNAi

RNAi experiments were conducted as previously described (Zhou *et al.* 2014). Synchronized embryos were grown on *unc-15* RNAi plates, and phenotypes were scored 3 days later. Bacteria expressing the *unc-15* dsRNA were obtained from the Ahringer RNAi library and sequenced to verify their identity (Kamath *et al.* 2003).

Benomyl assays

The benomyl assay was conducted as previously described (Driscoll *et al.* 1989). Briefly, synchronized embryos were grown on NGM plates supplemented with 14 μM benomyl (Sigma) and maintained at 25° for 2 days. Sensitivity to benomyl was assessed by scoring the movement and body shape of the animals.

Egg-hatching assay

Egg-hatching assays were performed as previously described (Herman 1978; Rosenbluth and Baillie 1981). Hermaphrodites were placed on NGM plates containing 6- to 10-mm diameter bacterial lawns and allowed to lay eggs for 3–4 hr, then the animals were picked off, and the eggs were counted. Three days later, the number of animals on the plates was counted again.

Results

Cas9 directs chromosomal translocation between dpy-13 (LG IV) and rde-12 (LG V)

To test whether Cas9 could direct chromosomal translocation in *C. elegans*, we simultaneously injected sgRNAs targeting

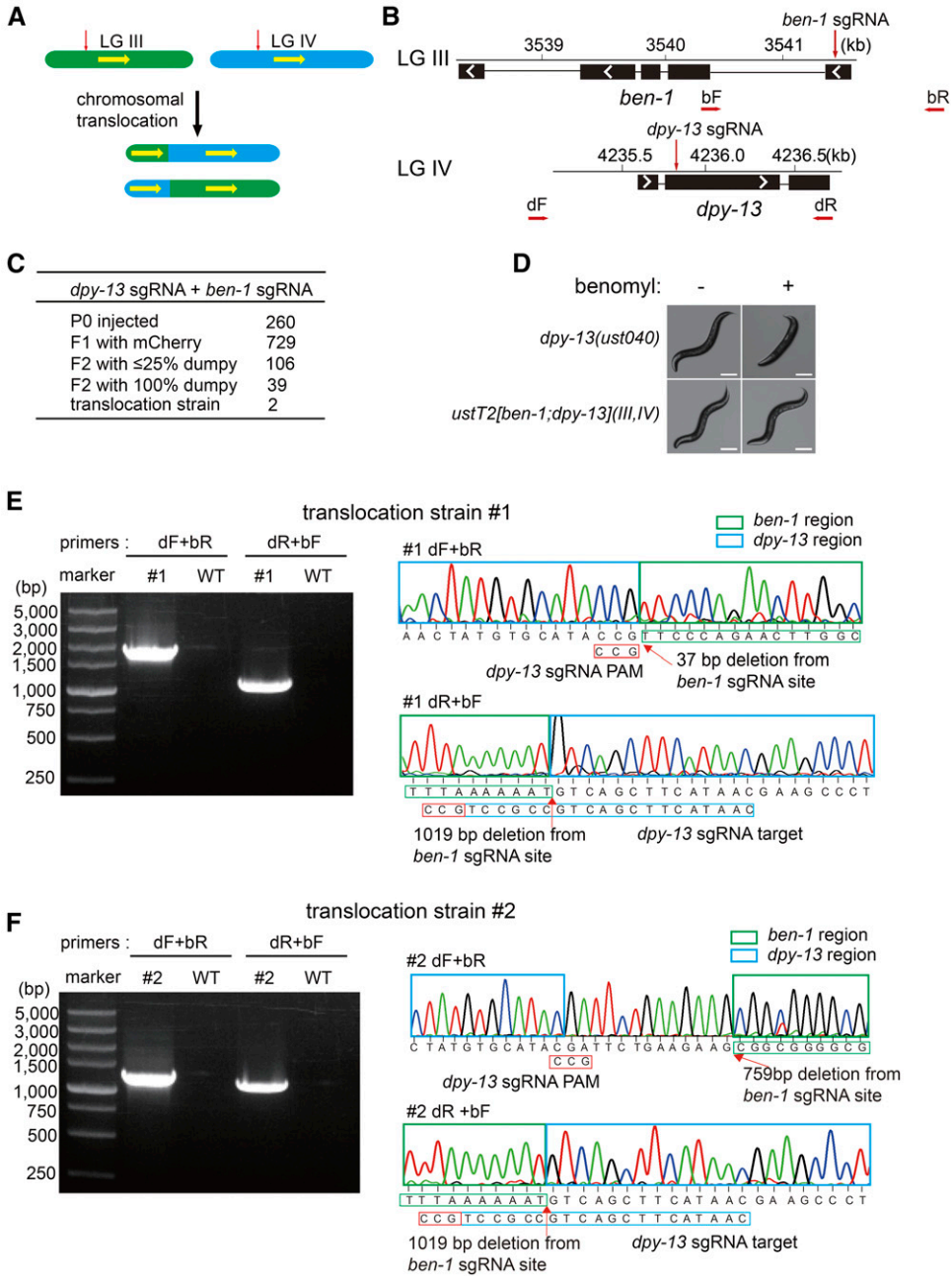

Figure 2 Cas9 directs chromosome translocation between *ben-1 (LG III)* and *dpy-13 (LG IV)*. (A) Schematic depicting the overall strategy of generating chromosomal rearrangements. The red arrows indicate the sgRNA targets, and the yellow arrows show the orientation of the chromosomes. (B) Schematic of the *ben-1* and *dpy-13* genes. Positions of sgRNA-guided cleavage sites and PCR primers for genotyping are indicated. (C) Summary of the microinjection experiments. (D) The chromosomal translocation strain *ustT2[ben-1;dpy-13](III,IV)* is benomyl-resistant. (E and F) PCR detection (left) and chromatogram of DNA sequencing (right) of the *ustT2(IV)* and *ustT2(III)* chromosomes of mutants #1 and #2. Breakpoints and sgRNA targets are indicated. Bars, 100 μm.

dpy-13 and *rde-12* (Figure 1, A and B). *dpy-13* is a collagen gene localized on LG IV, and *dpy-13* mutant animals exhibit a dumpy morphology (Zhou *et al.* 2014). The *rde-12* gene is localized on LG V and encodes an RNA helicase that engages targeted messenger RNA and Argonaute proteins to promote the synthesis of secondary small interfering RNAs in *C. elegans* (Shirayama *et al.* 2014; Yang *et al.* 2014). The loss of function of *rde-12* results in resistance to exo-RNAi.

To trigger chromosomal translocation between different genomic loci by the CRISPR/Cas9 technology, these two loci needed to be cleaved concurrently and repaired through the NHEJ pathway (Ghezraoui *et al.* 2014). This process requires sgRNAs with high efficiency to engage the CRISPR/Cas9 system and trigger DNA cleavage. Therefore, first we compared a number of sgRNAs targeting the *dpy-13* and *rde-12* loci. For *dpy-13*, three sgRNAs were designed and the gene editing efficiency of each sgRNA was assessed by phenotype analysis (Figure S1). sgRNA #2 targeting exon 2 of the *dpy-13* gene exhibited the highest efficiency and was used in the translocation experiments. For *rde-12*, the sgRNA targeting exon 2 of *rde-12* was previously reported to have a high cleavage efficiency (Chen *et al.* 2014) and was used in this work.

We co-injected sgRNAs targeting *rde-12* and *dpy-13* with Cas9 and mCherry expression plasmids into *eri-1(mg366)* animals (Figure S2). The mutation of *eri-1* results in an enhanced RNAi (Eri) phenotype that facilitates the analysis of

exo-RNAi sensitivity (Zhou *et al.* 2014). The loss of function of *rde-12* results in resistance to exo-RNAi. mCherry was used as a co-injection marker. From the 150 injected animals, we obtained 369 fertile F1 animals expressing mCherry that were subsequently singly transferred to individual NGM plates to produce F2 progeny. We searched for translocation mutants by analyzing the dumpy phenotype of F2 animals and PCR screening. From the 369 F1 animals, 32 produced F2 progeny in which ~25% were dumpy, and two F1 animals produced 100% dumpy F2 progeny (Figure 1C). The dumpy animals were selected and examined by PCR to search for mutants with chromosomal translocations. We successfully identified one mutant with reciprocal chromosomal translocation between *dpy-13* and *rde-12*. This mutant exhibited both the dumpy and the RNAi defective phenotypes (Figure 1D and Figure S3). Interestingly, this mutant belonged to the group of the two F1 animals that produced 100% dumpy F2 progeny. The translocated chromosomes were further confirmed by DNA sequencing (Figure 1, E and F).

Using the CRISPR/Cas9 system to direct chromosomal translocation between ben-1 (LG III) and dpy-13 (LG IV)

To further test the Cas9-directed chromosomal translocation strategy, we co-injected two sgRNAs targeting *dpy-13* and *ben-1* (Figure 2, A and B). The *ben-1* gene is localized on LG III and encodes a β-tubulin gene that confers benomyl (an antimicrotubule drug) sensitivity. Wild-type animals exposed to benomyl at 25° exhibit slow growth and a paralysis phenotype that is not observed in *ben-1* mutants (Driscoll *et al.* 1989). An sgRNA targeting *ben-1* with a high cleavage efficiency was previously reported (Figure 2B) (Chen *et al.* 2013).

We co-injected the sgRNAs targeting *dpy-13* and *ben-1* with the Cas9 and mCherry expression plasmids into wild-type animals. From 260 injected animals, we obtained 729 fertile F1 animals expressing mCherry. After these animals were singly transferred to NGM plates, they laid F2 progeny. We searched for the translocation mutants by analyzing the dumpy animals. From the 729 F1 animals, 106 produced F2 progeny in which ~25% were dumpy; additionally, 39 F1 animals produced 100% dumpy F2 progeny (Figure 2C). We successfully isolated two chromosomal translocation strains that exhibited the dumpy phenotype and failed to respond to benomyl (Figure 2D). Strikingly, these two mutants also belonged to the group of the 39 F1 animals that produced 100% dumpy F2 animals. The chromosomal translocation was further confirmed by DNA sequencing (Figure 2, E and F). Interestingly, these two mutants arose from the same F1, and the sequence of one of the translocated chromosomes was identical.

Pseudolinkage analysis and egg-hatching assay

To further demonstrate that the two chromosomal translocation strains contain the expected chromosome fusions, we conducted genetic analysis to test the presence of pseudolinkage between the two alleles generated by chromosomal translocations (Herman 1978; Rosenbluth and Baillie 1981). The strain *ustT1[dpy-13;rde-12](IV, V)* was generated via the cross of the strain *ustT1[eri-1(mg366);dpy-13;rde-12](IV, V)* with the wild-type N2 strain and was used in the following assays. *ustT1* is short for the strain *ustT1[dpy-13;rde-12](IV, V)*, and *ustT2* is short for the strain *ustT2[ben-1;dpy-13](III IV)* in the text.

Table 1 Egg-hatching assay and number of progeny

Genotype of parental hermaphrodite	% eggs reaching adulthood (%)[a]	Mean no. of adult progeny per hermaphrodite[b]
+/+	99.7 (661)	298 (10)
ustT1	96.7 (522)	147 (10)
ustT2	99.5 (407)	223 (10)
+/*ustT1*	36.2 (883)	101 (10)
+/*ustT2*	37.2 (1186)	105 (10)
+/*ustT2 [ben-1] III*; *unc-30(e191)/ustT2 [dpy-13] IV*	37.7 (917)	109 (14)

[a] Determined as described by Herman (1978). The total number of eggs counted is in parentheses.
[b] The numbers of parent hermaphrodites are in parentheses.

We tested the pseudolinkage between mutant alleles of *dpy-13* and *rde-12* in the *ustT1[dpy-13;rde-12](IV, V)* strain. *ustT1* hermaphrodites were crossed with wild-type N2 strain, and the F1 gravid adult animals were singled to *unc-15* RNAi plates. Among >400 F2 animals that suppressed *unc-15* RNAi (because of the mutation in *rde-12*), 100% of them displayed a dumpy morphology. Meanwhile, we transferred F1 animals to NGM plates to lay F2 progeny and singled >200 dumpy F2 animals to *unc-15* RNAi plates. All the F3 progeny generated by the dumpy F2 animals suppressed *unc-15* RNAi and failed to exhibit paralysis (which is induced by *unc-15* RNAi). These data support the presence of a pseudolinkage between *dpy-13(ustT1)* and *rde-12(ustT1)* and that *ustT1* carries a translocation between LG IV and LG V.

We tested the pseudolinkage between mutant alleles of *dpy-13* and *ben-1* in *ustT2[ben-1;dpy-13](III,IV)*. *ustT2* hermaphrodites were crossed with wild-type N2 strain, and the F1 gravid adult animals were singled to NGM plates to lay F2 progeny. More than 200 dumpy F2 gravid adults were singled to benomyl-containing plates. All the F3 progeny exhibited resistance to the benomyl treatment and failed to display uncoordinated phenotype (which is induced by benomyl). This evidence supports the presence of a pseudolinkage between *dpy-13(ustT2)* and *ben-1(ustT2)* and that *ustT2* carries a translocation between LG III and LG IV.

The chromosomal translocations were further confirmed by egg-hatching assays of the +/*ustT1* and +/*ustT2* heterozygous strains (Table 1). For eggs from the +/*ustT1* and +/*ustT2* hermaphrodites, it is expected that 37.5% of them could reach adulthood (Herman 1978; Rosenbluth and Baillie 1981). The actual egg-surviving rates of +/*ustT1* and +/*ustT2* heterozygotes were 36.2% (n = 883) and 37.2%

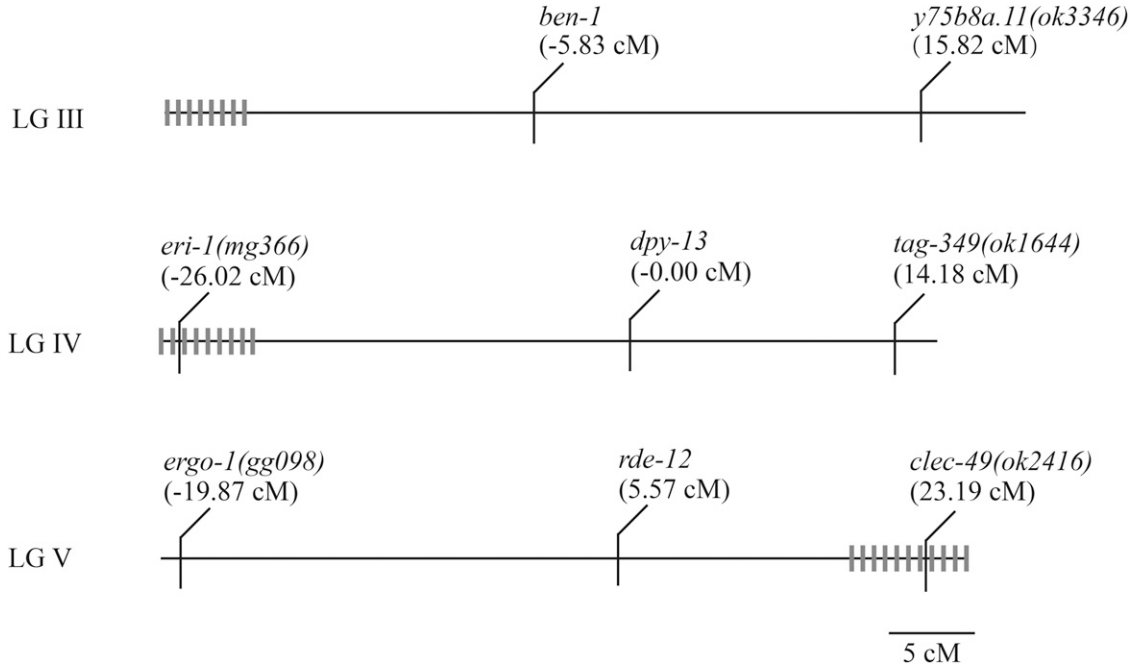

Figure 3 The relative position of selected alleles used to map the recombination suppression regions. The gray vertical lines indicate the pairing center (Rog and Dernburg 2013).

(n = 1186), respectively, which agreed well with the predicted value.

Chromosomal translocation suppresses recombination in the nonpairing center regions

Each of the six chromosomes of *C. elegans* contains a pairing center, which locates asymmetrically near one end and mediates homologous chromosome pairing and segregation during meiosis (Rog and Dernburg 2013). Chromosomes that contain homologous PC regions can pair with each other and undergo synapsis along their lengths, regardless of the nonhomologous chromosomal regions. However, chromosomes lacking these regions will fail to pair and synapse with their homologs. Chromosomal translocations have profound effects on the process of synapsis and recombination during meiosis. In heterozygotes carrying normal and translocated chromosomes, the crossover process occurs normally among the chromosomal regions from the nonpairing center (PC) end to the fusion point and is suppressed from the fusion point to the nonpairing center end of the chromosome (Herman 1978; Rosenbluth and Baillie 1981; Rog and Dernburg 2013). We examined the recombination capability of different chromosomal regions of *ustT1* and *ustT2* by crossing them with a series of mutants that carry marker alleles on LG III, LG IV, and LG V, respectively (Figure 3 and Table 2). These marker alleles are all indels, which localize near the ends of each chromosome and can be easily genotyped by PCR amplification. As controls, we also crossed these marker strains with control animals that have normal chromosome sets but carry alleles in *dpy-13(ust40)* or *rde-12(ust17)*. The primers used for genotyping these indels are listed in Table S5.

The *eri-1* locus maps to LG IV: −26.02 in the pairing center, which is on the left arm to *dpy-13* (Figure 3). We crossed *eri-1(mg366)* with *dpy-13(ust40)*, selected dumpy F2 animals, and genotyped the presence of the *eri-1(mg366)* allele by single-worm PCR amplification. The recombination frequency was calculated by dividing the number of F2 dumpy animals carrying the *eri-1(mg366)* allele by the number of total F2 animals. Crossing *eri-1(mg366)* with *dpy-13(ust40)* resulted in a 12.6% recombination frequency (n = 1635 total F2 animals) (Table 2). Crossing *eri-1(mg366)* with *ustT1* and *ustT2* resulted in 12.4% and 12.5% recombination, respectively. The *tag-349* locus maps to LG IV:14.18, distal to the pairing center, which is on the right arm to *dpy-13*. Crossing *tag-349(ok1644)* with *dpy-13(ust40)* generated 6.9% recombination. However, crossing *tag-349(ok1644)* with *ustT1* and *ustT2* did not produce any recombination (n = 1680 and 2205 total F2 animals, respectively). These results suggest that the chromosomal translocations do not suppress recombination in the chromosomal region from *dpy-13* to the left end of LG IV, but suppress the recombination from *dpy-13* to the right end of LG IV.

ergo-1 localizes near the left end of LG V, and *clec-49* localizes near the right end of LG V. The chromosomal translocation in *ustT1* suppressed the recombination in the region between *ergo-1* and *rde-12*, yet it did not suppress the recombination in the region between *clec-49* and *rde-12* (Table 2). *y75b8a.11* localizes near the right end of LG III. We did not get any recombinants between *y78b8a.11* and *ben-1* from a total of 1207 F2 animals when crossing *y75b8a.11(ok3346)* with *ustT2*, suggesting that the recombination in the region from *ben-1* to the right end of LG III is suppressed by chromosomal translocations.

Table 2 Recombination capability of different chromosomal regions of *ustT1* and *ustT2*

Male[a]	Hermaphrodite[a]	PCR markers (gene allele)	Frequencies of recombinants (total adult progeny) Dpy or Rde animals with PCR markers
GR1373 (*eri-1(mg366)*)	SHG373 (*dpy-13(ust40)*)	*mg366*	0.126 (1635)
GR1373 (*eri-1(mg366)*)	SHG374 (*ustT1[dpy-13] IV;ustT1[rde-12] V*)	*mg366*	0.124 (1589)
GR1373 (*eri-1(mg366)*)	SHG375 (*ustT2[ben-1] III;ustT2[dpy-13]IV*)	*mg366*	0.125 (2387)
RB1441 (*tag-349(ok1644)*)	SHG373 (*dpy-13(ust40)*)	*ok1644*	0.069 (689)
RB1441 (*tag-349(ok1644)*)	SHG374 (*ustT1[dpy-13] IV;ustT1[rde-12] V*)	*ok1644*	0 (1680)
RB1441 (*tag-349(ok1644)*)	SHG375 (*ustT2[ben-1] III;ustT2[dpy-13]IV*)	*ok1644*	0 (2205)
YY166 (*ergo-1(gg98)*)	SHG376 (*rde-12(ust17)*)	*gg98*	0.125 (768)[b]
YY166 (*ergo-1(gg98)*)	SHG374 (*ustT1[dpy-13] IV;ustT1[rde-12] V*)	*gg98*	0 (1487)[b]
RB1870 (*clec-49(ok2416)*)	SHG376 (*rde-12(ust17)*)	*ok2416*	0.102 (740)[b]
RB1870 (*clec-49(ok2416)*)	SHG375 (*ustT2[ben-1] III;ustT2[dpy-13]IV*)	*ok2416*	0.110 (556)[b]
VC2575 (*y75b8a.11(ok3346)*)	SHG375 (*ustT2[ben-1] III;ustT2[dpy-13]IV*)	*ok3346*	0 (1207)

[a] The genotypes of the strains are showed in parentheses.
[b] The F2 animals suppressing *unc-15* RNAi treatment were singled out and genotyped.

We conclude, for *ustT1*, that recombination is suppressed from *dpy-13* to the right end of LG IV and from *rde-12* to the left end of LG V, yet recombination is not suppressed from the left end to *dpy-13* on LG IV and from the right end to *rde-12* on LG V. For *ustT2*, recombination is suppressed from *ben-1* to the right end of LG III and from *dpy-13* to the right end of LG IV. These results are consistent with the localization of pairing centers on each chromosome (Rog and Dernburg 2013). Recombination occurs normally in the regions containing pairing centers, while it is suppressed in the translocated chromosome regions without pairing centers.

Schematic of balancer construction of essential genes

Nematode strains with special chromosomal rearrangements have been used to construct genetic balancers of essential genes (Edgley *et al.* 2006; Jones *et al.* 2011). Here, we developed a new method to generate and maintain the loss-of-function alleles of essential genes by integrating the CRISPR/Cas9 technology with the balancer system (Figure 4). The *ustT2[ben-1;dpy-13](III,IV)* strain, which was generated in Figure 2 and carried a reciprocal translocation between LG III and LG IV, was used to illustrate this method.

First, we crossed *ustT2[ben-1;dpy-13](III,IV)* and CB845: *unc-30(e191)* to generate F1 heterozygous progeny. CB845 carries an *unc-30(e191)* allele to facilitate the screening and maintenance of mutants with the Unc morphology marker. The F1 heterozygotes were injected with the Cas9 expression plasmid, GFP expression plasmid, and the plasmids expressing sgRNAs targeting the lethal *gene X*. Both copies of *gene X* on the two chromosomes can be edited. The F1 animals generated F2 progeny with a segregation of Dpy, Unc, and the wild-type morphology (Figure S4, File S1). The F2 animals with wild-type morphology and GFP expression were singly transferred to individual NGM plates to lay F3 progeny, which exhibited a Dpy, Unc, lethal, or wild-type phenotype. By analyzing the linkage between lethality and the Dpy or Unc phenotype, the alleles of essential *gene X* can be identified. The presence of the *dpy-13* or *unc-30* alleles further simplified the identification and maintenance of the chromosomes on which the alleles of gene *X* were localized. Additionally, mutants with large sequence deletions can be easily pinpointed by PCR-based single-worm genotyping of the F2 animals.

We examined the phenotypic segregation ratio of the *unc-30(e191)/ustT2* heterozygote, which is expected to be 4:1:1 of wild-type:Dpy:Unc animals within the progeny (Figure S4). Among a total of 1706 progeny, we observed 1148 wild-type, 282 Dpy, and 276 Unc individuals, which exhibited a ratio of 4.16:1.02:1 that agreed well with the expectation.

Balancer construction of csr-1 using the CRISPR/Cas9 system

CSR-1 is a germline-expressed Argonaute protein that is required for faithful chromosome segregation and embryonic viability (Claycomb *et al.* 2009). The homozygous *csr-1* mutants are sterile, although they produce a very few embryos with chromosome segregation defects.

The strain *ustT2[ben-1;dpy-13](III,IV)* was first crossed with CB845:*unc-30(e191)*. Then, we co-injected three sgRNA expression vectors targeting exons 2 and 4 of *csr-1* with the Cas9 and GFP expression plasmids into the F1 heterozygous animals (Figure 5A and Figure S5A). From the 90 injected F1 animals, we acquired 155 fertile F2 animals with wild-type morphology and GFP expression (Figure 5B). F2 animals were singly transferred to individual NGM plates to lay F3 progeny. From the 155 F2 animals, 5 produced F3 animals with linkage between the uncoordinated and sterile phenotypes, and 2 F2 animals produced F3 animals with linkage between the dumpy and sterile phenotypes. The linkage between the sterile phenotype and morphological markers indicated the chromosome on which the mutations were located (Figure S5B). Interestingly, 3 F2 animals with large deletions were directly screened out via single-worm PCR of the F2 animals (Figure 5C). The *csr-1* alleles were confirmed by PCR amplification and sequencing (Figure 5, D and E).

One of the balancer strains, *+/ustT2 [ben-1] III;csr-1(ust41) unc-30(e191) IV/ustT2 [dpy-13] IV*, which carries a *csr-1(ust41)* mutation on the normal chromosome, was

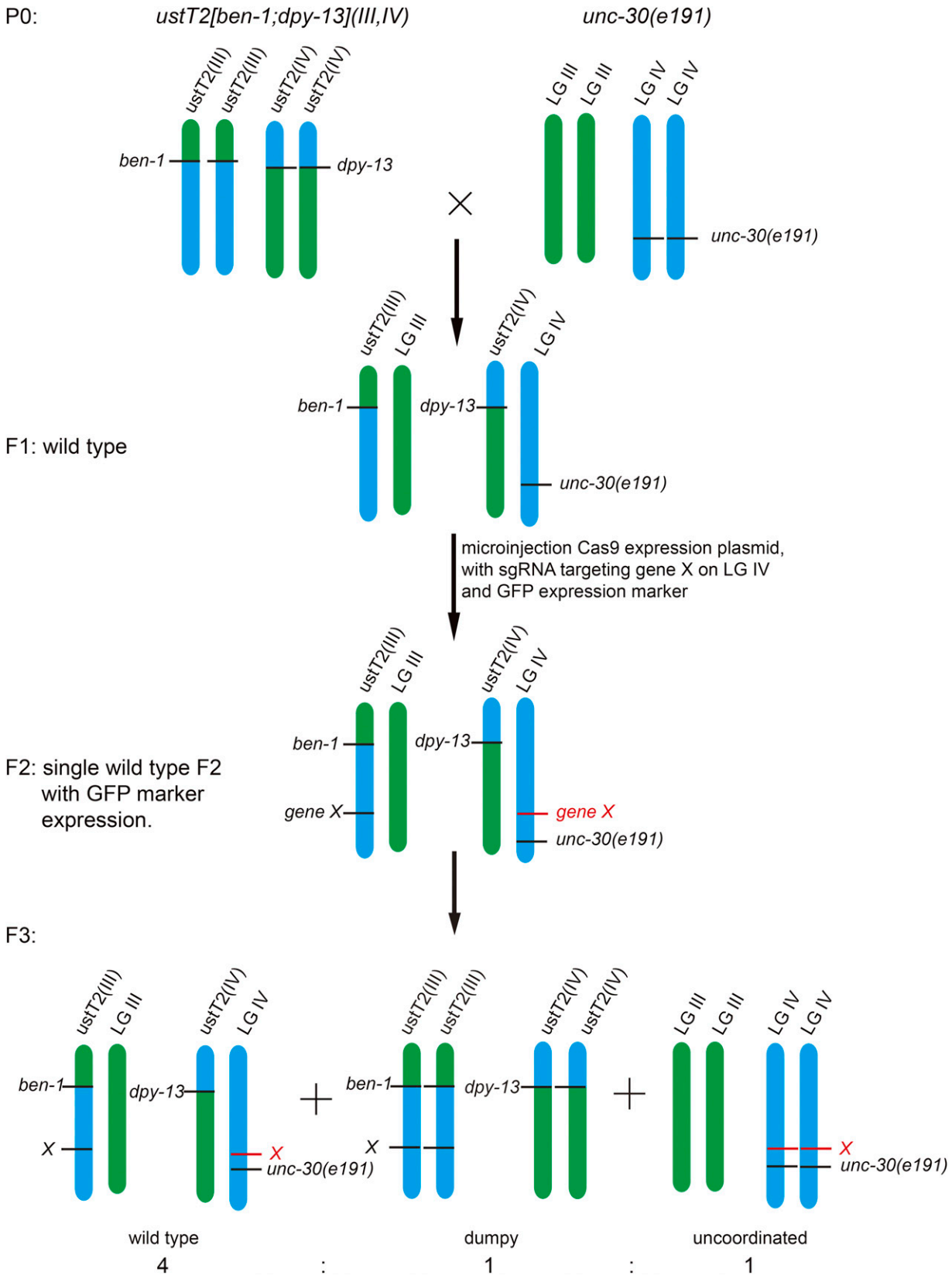

Figure 4 Schematic of the balancer construction of the lethal *gene X*. The F1 heterozygous strain was generated by the mating of *ustT2[ben-1;dpy-13](III,IV)* with *unc-30(e191)* and was subjected to the microinjection of sgRNA and Cas9 expression plasmids. Both copies of the lethal *gene X* can be edited. The allele on the wild-type chromosome is marked with red color, and the allele on the translocated chromosome is marked with black color.

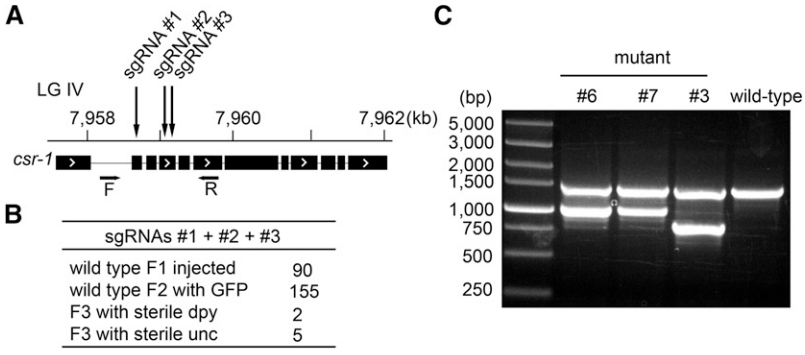

B

sgRNAs #1 + #2 + #3	
wild type F1 injected	90
wild type F2 with GFP	155
F3 with sterile dpy	2
F3 with sterile unc	5

D

F3 with sterile unc

```
wild-type   ATTTCAGAGGACGTGGAAACCGTGCAACAAAGCATAAAGA
mutant #1   ATTTCAGAGGACGTG-tAACCGTGCAACAAAGCATAAAGA (+1bp,-2bp)

wild-type   AACATTGAACAAAGG(692bp)GCGGCGATTTGGAGATCT
mutant #3   AACATTGAACAAAGG-------GCGGCGATTTGGAGATCT (-692bp)

wild-type   CCAATTTTCTGAAGG(33bp)TCTCTTGTGAACCGGATCT
mutant #4   CCAATTTTCTGAAGG------TCTCTTGTGAACCGGATCT (-33bp)

wild-type   TGTATTTGGGTTTAT(478bp)ATTCAATCCCACTCAGTC
mutant #6   TGTATTTGGGT---gtcagatgttgagt----ACTCAGTC (+15bp,-492bp)

wild-type   AGGATTCCATCTCGT(464bp)TATCGTTAATCCAAATAT
mutant #7   AGGATTCCATCTCGT-------TATCGTTAATCCAAATAT (-464bp)
```

E

F3 with sterile dpy

```
wild-type   TCTGAAGGATTCCATCTCGTTCCTCGTTCCTCAGCGGCGA
mutant #2   TCTGAAGGATTCCAT-------CTCGTTCCTCAGCGGCGA (-7bp)

wild-type   TGAAGGATTCCATCTCGTTCCTCAGCGGCGATTTGGAGAT
mutant #5   TGAAGGATTCCATCT-----CTCAGCGGCGATTTGGAGAT (-5bp)
```

Figure 5 The gene editing and balancer construction of *csr-1* using the CRISPR/Cas9 technology. (A) Schematic of the *csr-1* gene. The sgRNA-targeted sites and the PCR primers for genotyping are indicated. (B) Summary of the microinjection experiments. (C) Single-worm PCR detection of the examples of the balanced F2 mutants. (D and E) Sequence alignments of wild-type and mutant animals with sterile uncoordinated and sterile dumpy phenotypes. The dashes indicate a deletion. The numbers in parentheses within the sequence represent the number of bases not shown. The number of deleted (−) or inserted (+) bases is indicated to the right of each indel.

examined to verify its linkage with *unc-30(e191)*. L4 heterozygous *+/ustT2 [ben-1] III;csr-1(ust41) unc-30(e191) IV/ustT2 [dpy-13] IV* animals were singled to NGM plates to lay eggs. Three days later, >800 uncoordinated larva animals were singly transferred to new NGM plates, and their fertility was scored after another 4–5 days. We observed only a few dead embryos but no viable larva progeny from these 800 uncoordinated parents, which is consistent with the sterility of the *csr-1* homozygous mutation.

Therefore, these loss-of-function *csr-1* alleles were balanced with the translocation of chromosomal *ustT2[dpy-13] (IV)* and maintained as heterozygous states.

Genetic balancer generation of mes-6

MES-6 is a member of the polycomb-like chromatin repressive complex (PRC2) (Xu *et al.* 2001) that is engaged in germline development and regulation of gene expression. The loss of function of *mes-6* results in a maternal sterile phenotype in which the heterozygous mother produces 25% homozygous *mes* progeny that are themselves fertile but produce sterile progeny.

The strain *ustT2[ben-1;dpy-13](III,IV)* was first crossed with *unc-30(e191)*. Then we co-injected three sgRNA expression plasmids targeting exons 1 and 2 of *mes-6* with the Cas9 and GFP expression plasmids into the F1 heterozygous animals (Figure 6A and Figure S6A). From 100 injected F1 animals, we obtained 165 fertile F2 animals expressing GFP with wild-type morphology (Figure 6B). F2 animals were singly transferred to NGM plates to lay F3 progeny. From each plate, 6–8 dumpy or uncoordinated animals were transferred to individual NGM plates to lay F4 progeny. From the total of 165 F2 animals, 17 produced F4 progeny with a linkage between the Dpy and maternal sterile phenotypes, 20 F2 progeny produced F4 progeny with a linkage between the uncoordinated and sterile phenotypes, and 13 F2 animals produced sterile F3 animals with both the Dpy and the Unc phenotypes. The linkage between sterility and the morphological phenotypes indicated the chromosome on which the mutations were located (Figure S6B). Interestingly, 2 F2 animals with large deletions were directly screened out via single-worm PCR of the F2 animals (Figure 6C). The *mes-6* alleles of a subset of these mutants were verified by PCR and sequencing (Figure 6, D–F). Therefore, these loss-of-function *mes-6* alleles were balanced with the translocation of chromosomal *ustT2[dpy-13] (IV)* and maintained in heterozygous state.

Discussion

Recurrent chromosomal translocations in mammalian cells usually result in chimeric fusion transcripts that lead to the expression of fusion proteins and drive oncogenesis. A series of technologies have been developed to establish cancer models by inducing chromosomal translocation in cell lines. These technologies include the rare-cutting I-SceI endonuclease (Richardson and Jasin 2000), zinc finger nucleases, TALE nucleases, and the CRISPR/Cas9 system, all of which are able to introduce DSBs into distinct chromosomal loci and

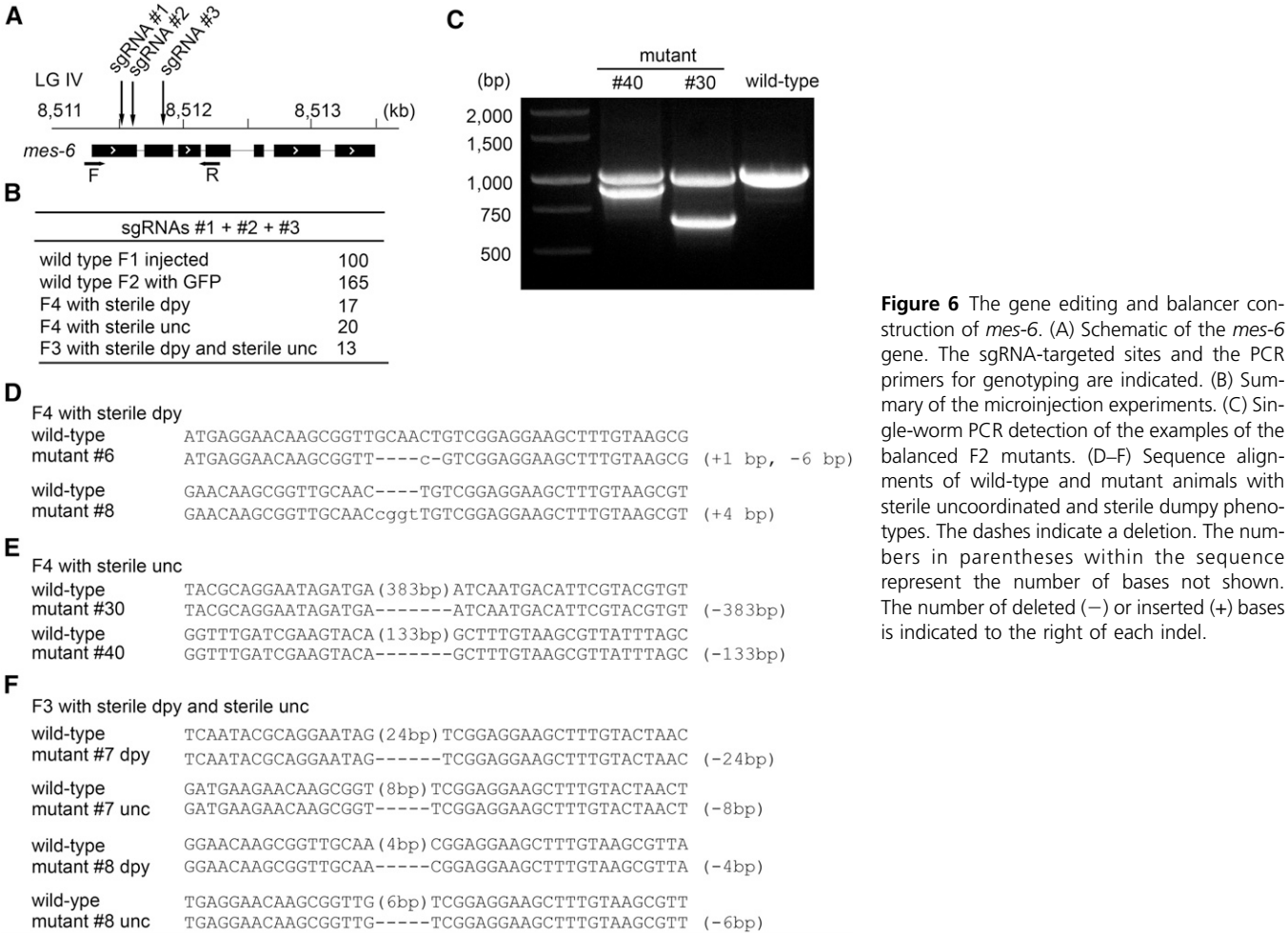

Figure 6 The gene editing and balancer construction of *mes-6*. (A) Schematic of the *mes-6* gene. The sgRNA-targeted sites and the PCR primers for genotyping are indicated. (B) Summary of the microinjection experiments. (C) Single-worm PCR detection of the examples of the balanced F2 mutants. (D–F) Sequence alignments of wild-type and mutant animals with sterile uncoordinated and sterile dumpy phenotypes. The dashes indicate a deletion. The numbers in parentheses within the sequence represent the number of bases not shown. The number of deleted (−) or inserted (+) bases is indicated to the right of each indel.

generate translocated chromosomes by NHEJ. In *C. elegans*, a number of strains with chromosomal rearrangements were previously generated using mutagenic chemicals or irradiation. However, these traditional methods are time-consuming, laborious, and rarely achieve specific rearrangements on purpose. Additionally, many unintended mutations can be introduced into the genome by mutagenesis. Here, we developed a method using the CRISPR/Cas9 technology to direct chromosomal translocations in *C. elegans*. Through the co-injection of sgRNAs targeting different chromosomes, designated chromosomal translocation strains with nominal off-target mutations were constructed rapidly and efficiently.

Targeted chromosomal translocations are beneficial for many studies, such as meiotic processes. *C. elegans* chromosomes contain specialized regions called pairing centers that localize at the end of each chromosome and mediate homologous pairing and synapsis during meiosis (MacQueen *et al.* 2005; Phillips and Dernburg 2006; Phillips *et al.* 2009; Rog and Dernburg 2013). However, the detailed sequence information and mechanisms involved with the pairing centers remain unclear. Using the CRISPR/Cas9 technology to generate specific chromosomal translocations will help to pin point these regions and illuminate the mechanisms underlying homolog pairing, synapsis, and segregation during meiosis.

Balancers are genetic constructs or chromosomal rearrangements that allow lethal or sterile mutations to be stably maintained in heterozygotes (Hackstein *et al.* 1992; Zheng *et al.* 1999; Chick *et al.* 2004; Hentges and Justice 2004). Balancers can be applied to a variety of tasks, including construction of strains, maintenance of mutations, and screening for new mutants. Conventional methods using existing balancer strains to screen and maintain the alleles of essential genes are very cumbersome and time-consuming. In this work, we developed a rapid and efficient method using the CRISPR/Cas9 technology to directly generate balancer strains with loss-of-function alleles of essential genes. Starting from the initial cross, the experiment can be finished within 10 days and is able to generate many alleles of the targeted genes. Moreover, by using multiple sgRNAs in the microinjection experiment followed by genotyping of the F2s with PCR detection, we can easily isolate deletion alleles of the targeted genes.

Linking lethality to morphological markers is especially helpful for experiments because it is much easier to score for the presence of a particular morphological phenotype than to

score arrested embryos or larvae. The chromosomal translocation strains generated in this work carry *dpy-13*, *rde-12*, or *ben-1* mutations. We also introduced the *unc-30(e191)* allele in the mating step prior to the microinjection of the Cas9 expression plasmid. These markers eased the manipulation of genetic crosses and the selection of homozygous mutants. Other markers or GFP reporters can also be included in the mating step, which will benefit the study of the balanced genes.

In summary, our work provides a novel platform with which to use the CRISPR/Cas9 technology to generate nematode strains with specified chromosomal translocations and produce and maintain loss-of-function alleles of essential genes via the balancer system. This method is also applicable to studying essential genes in other organisms.

Acknowledgments

We thank members of the Guang lab for their comments and the *Caenorhabditis* Genetics Center, the International *C. elegans* Gene Knockout Consortium, and the National Bioresource Project for providing the strains. This work was supported by grants from the National Natural Science Foundation of China (nos. 31171254 and 31371323), the Fundamental Research Funds for Central Universities (nos. WK2060190018, WK2070000034, and KJZD-EW-L01-2).

Literature Cited

Arribere, J. A., R. T. Bell, B. X. Fu, K. L. Artiles, P. S. Hartman *et al.*, 2014 Efficient marker-free recovery of custom genetic modifications with CRISPR/Cas9 in *Caenorhabditis elegans*. Genetics 198: 837–846.

Brenner, S., 1974 The genetics of *Caenorhabditis elegans*. Genetics 77: 71–94.

Chen, C., L. A. Fenk, and M. de Bono, 2013 Efficient genome editing in *Caenorhabditis elegans* by CRISPR-targeted homologous recombination. Nucleic Acids Res. 41: e193.

Chen, X., F. Xu, C. Zhu, J. Ji, X. Zhou *et al.*, 2014 Dual sgRNA-directed gene knockout using CRISPR/Cas9 technology in *Caenorhabditis elegans*. Sci. Rep. 4: 7581.

Chick, W. S., S. E. Mentzer, D. A. Carpenter, E. M. Rinchik, and Y. You, 2004 Modification of an existing chromosomal inversion to engineer a balancer for mouse chromosome 15. Genetics 167: 889–895.

Chiu, H., H. T. Schwartz, I. Antoshechkin, and P. W. Sternberg, 2013 Transgene-free genome editing in *Caenorhabditis elegans* using CRISPR-Cas. Genetics 195: 1167–1171.

Cho, S. W., J. Lee, D. Carroll, J. S. Kim, and J. Lee, 2013 Heritable gene knockout in *Caenorhabditis elegans* by direct injection of Cas9-sgRNA ribonucleoproteins. Genetics 195: 1177–1180.

Choi, P. S., and M. Meyerson, 2014 Targeted genomic rearrangements using CRISPR/Cas technology. Nat. Commun. 5: 3728.

Claycomb, J. M., P. J. Batista, K. M. Pang, W. Gu, J. J. Vasale *et al.*, 2009 The Argonaute CSR-1 and its 22G-RNA cofactors are required for holocentric chromosome segregation. Cell 139: 123–134.

Cong, L., F. A. Ran, D. Cox, S. Lin, R. Barretto *et al.*, 2013 Multiplex genome engineering using CRISPR/Cas systems. Science 339: 819–823.

Dickinson, D. J., J. D. Ward, D. J. Reiner, and B. Goldstein, 2013 Engineering the *Caenorhabditis elegans* genome using Cas9-triggered homologous recombination. Nat. Methods 10: 1028–1034.

Driscoll, M., E. Dean, E. Reilly, E. Bergholz, and M. Chalfie, 1989 Genetic and molecular analysis of a *Caenorhabditis elegans* beta-tubulin that conveys benzimidazole sensitivity. J. Cell Biol. 109: 2993–3003.

Edgley, M. L., D. L. Baillie, D. L. Riddle, and A. M. Rose, 2006 Genetic balancers. Genetic balancers (April 6, 2006), WormBook, ed. The *C. elegans* Research Community, WormBook, doi/10.1895/wormbook.1.89.1, http://www.wormbook.org.

Farboud, B., and B. J. Meyer, 2015 Dramatic enhancement of genome editing by CRISPR/Cas9 through improved guide RNA design. Genetics 199: 959–971.

Friedland, A. E., Y. B. Tzur, K. M. Esvelt, M. P. Colaiacovo, G. M. Church *et al.*, 2013 Heritable genome editing in *C. elegans* via a CRISPR-Cas9 system. Nat. Methods 10: 741–743.

Frokjaer-Jensen, C., 2013 Exciting prospects for precise engineering of *Caenorhabditis elegans* genomes with CRISPR/Cas9. Genetics 195: 635–642.

Ghezraoui, H., M. Piganeau, B. Renouf, J. B. Renaud, A. Sallmyr *et al.*, 2014 Chromosomal translocations in human cells are generated by canonical nonhomologous end-joining. Mol. Cell 55: 829–842.

Hackstein, J. H., R. Hochstenbach, and F. M. van Breugel, 1992 Constructing balancer chromosomes for genetic screens in *Drosophila hydei*. Theor. Appl. Genet. 83: 821–826.

Hentges, K. E., and M. J. Justice, 2004 Checks and balancers: balancer chromosomes to facilitate genome annotation. Trends Genet. 20: 252–259.

Herman, R. K., 1978 Crossover suppressors and balanced recessive lethals in *Caenorhabditis elegans*. Genetics 88: 49–65.

Hsu, P. D., E. S. Lander, and F. Zhang, 2014 Development and applications of CRISPR-Cas9 for genome engineering. Cell 157: 1262–1278.

Jiang, W., D. Bikard, D. Cox, F. Zhang, and L. A. Marraffini, 2013 RNA-guided editing of bacterial genomes using CRISPR-Cas systems. Nat. Biotechnol. 31: 233–239.

Jones, M. R., Z. Lohn, and A. M. Rose, 2011 Specialized chromosomes and their uses in *Caenorhabditis elegans*. Methods Cell Biol. 106: 23–64.

Kamath, R. S., A. G. Fraser, Y. Dong, G. Poulin, R. Durbin *et al.*, 2003 Systematic functional analysis of the *Caenorhabditis elegans* genome using RNAi. Nature 421: 231–237.

Kannan, K., C. Coarfa, P. W. Chao, L. Luo, Y. Wang *et al.*, 2015 Recurrent BCAM-AKT2 fusion gene leads to a constitutively activated AKT2 fusion kinase in high-grade serous ovarian carcinoma. Proc. Natl. Acad. Sci. USA 112: E1272–E1277.

Katic, I., and H. Grosshans, 2013 Targeted heritable mutation and gene conversion by Cas9-CRISPR in *Caenorhabditis elegans*. Genetics 195: 1173–1176.

Kim, H., T. Ishidate, K. S. Ghanta, M. Seth, D. Conte, Jr. *et al.*, 2014 A co-CRISPR strategy for efficient genome editing in *Caenorhabditis elegans*. Genetics 197: 1069–1080.

Li, W., P. Yi, and G. Ou, 2015 Somatic CRISPR-Cas9-induced mutations reveal roles of embryonically essential dynein chains in *Caenorhabditis elegans* cilia. J. Cell Biol. 208: 683–692.

Lo, T. W., C. S. Pickle, S. Lin, E. J. Ralston, M. Gurling *et al.*, 2013 Precise and heritable genome editing in evolutionarily diverse nematodes using TALENs and CRISPR/Cas9 to engineer insertions and deletions. Genetics 195: 331–348.

MacQueen, A. J., C. M. Phillips, N. Bhalla, P. Weiser, A. M. Villeneuve *et al.*, 2005 Chromosome sites play dual roles to establish homologous synapsis during meiosis in *C. elegans*. Cell 123: 1037–1050.

Mali, P., L. Yang, K. M. Esvelt, J. Aach, M. Guell *et al.*, 2013 RNA-guided human genome engineering via Cas9. Science 339: 823–826.

Paix, A., Y. Wang, H. E. Smith, C. Y. Lee, D. Calidas *et al.*, 2014 Scalable and versatile genome editing using linear DNAs with microhomology to Cas9 sites in *Caenorhabditis elegans*. Genetics 198: 1347–1356.

Phillips, C. M., and A. F. Dernburg, 2006 A family of zinc-finger proteins is required for chromosome-specific pairing and synapsis during meiosis in *C. elegans*. Dev. Cell 11: 817–829.

Phillips, C. M., X. Meng, L. Zhang, J. H. Chretien, F. D. Urnov *et al.*, 2009 Identification of chromosome sequence motifs that mediate meiotic pairing and synapsis in *C. elegans*. Nat. Cell Biol. 11: 934–942.

Piganeau, M., H. Ghezraoui, A. De Cian, L. Guittat, M. Tomishima *et al.*, 2013 Cancer translocations in human cells induced by zinc finger and TALE nucleases. Genome Res. 23: 1182–1193.

Ran, F. A., P. D. Hsu, C. Y. Lin, J. S. Gootenberg, S. Konermann *et al.*, 2013 Double nicking by RNA-guided CRISPR Cas9 for enhanced genome editing specificity. Cell 154: 1380–1389.

Richardson, C., and M. Jasin, 2000 Frequent chromosomal translocations induced by DNA double-strand breaks. Nature 405: 697–700.

Rog, O., and A. F. Dernburg, 2013 Chromosome pairing and synapsis during *Caenorhabditis elegans meiosis*. Curr. Opin. Cell Biol. 25: 349–356.

Rosenbluth, R. E., and D. L. Baillie, 1981 The genetic analysis of a reciprocal translocation, eT1(III; V), in *Caenorhabditis elegans*. Genetics 99: 415–428.

Shalem, O., N. E. Sanjana, E. Hartenian, X. Shi, D. A. Scott *et al.*, 2014 Genome-scale CRISPR-Cas9 knockout screening in human cells. Science 343: 84–87.

Shirayama, M., W. Stanney, III, W. Gu, M. Seth, and C. C. Mello, 2014 The Vasa homolog RDE-12 engages target mRNA and multiple argonaute proteins to promote RNAi in *C. elegans*. Curr. Biol. 24: 845–851.

Sternberg, S. H., S. Redding, M. Jinek, E. C. Greene, and J. A. Doudna, 2014 DNA interrogation by the CRISPR RNA-guided endonuclease Cas9. Nature 507: 62–67.

Torres, R., M. C. Martin, A. Garcia, J. C. Cigudosa, J. C. Ramirez *et al.*, 2014 Engineering human tumour-associated chromosomal translocations with the RNA-guided CRISPR-Cas9 system. Nat. Commun. 5: 3964.

Waaijers, S., V. Portegijs, J. Kerver, B. B. Lemmens, M. Tijsterman *et al.*, 2013 CRISPR/Cas9-targeted mutagenesis in *Caenorhabditis elegans*. Genetics 195: 1187–1191.

Wang, H., H. Yang, C. S. Shivalila, M. M. Dawlaty, A. W. Cheng *et al.*, 2013 One-step generation of mice carrying mutations in multiple genes by CRISPR/Cas-mediated genome engineering. Cell 153: 910–918.

Wang, T., J. J. Wei, D. M. Sabatini, and E. S. Lander, 2014 Genetic screens in human cells using the CRISPR-Cas9 system. Science 343: 80–84.

Ward, J. D., 2015 Rapid and precise engineering of the *Caenorhabditis elegans* genome with lethal mutation co-conversion and inactivation of NHEJ repair. Genetics 199: 363–377.

Xu, L., Y. Fong, and S. Strome, 2001 The *Caenorhabditis elegans* maternal-effect sterile proteins, MES-2, MES-3, and MES-6, are associated in a complex in embryos. Proc. Natl. Acad. Sci. USA 98: 5061–5066.

Yang, H., J. Vallandingham, P. Shiu, H. Li, C. P. Hunter *et al.*, 2014 The DEAD box helicase RDE-12 promotes amplification of RNAi in cytoplasmic foci in *C. elegans*. Curr. Biol. 24: 832–838.

Zheng, B., M. Sage, W. W. Cai, D. M. Thompson, B. C. Tavsanli *et al.*, 1999 Engineering a mouse balancer chromosome. Nat. Genet. 22: 375–378.

Zhou, X., F. Xu, H. Mao, J. Ji, M. Yin *et al.*, 2014 Nuclear RNAi contributes to the silencing of off-target genes and repetitive sequences in *Caenorhabditis elegans*. Genetics 197: 121–132.

Communicating editor: B. Goldstein

GENETICS

Supporting Information
www.genetics.org/lookup/suppl/doi:10.1534/genetics.115.181883/-/DC1

Targeted Chromosomal Translocations and Essential Gene Knockout Using CRISPR/Cas9 Technology in *Caenorhabditis elegans*

Xiangyang Chen, Mu Li, Xuezhu Feng, and Shouhong Guang

DOI: 10.1534/genetics.115.181883

A

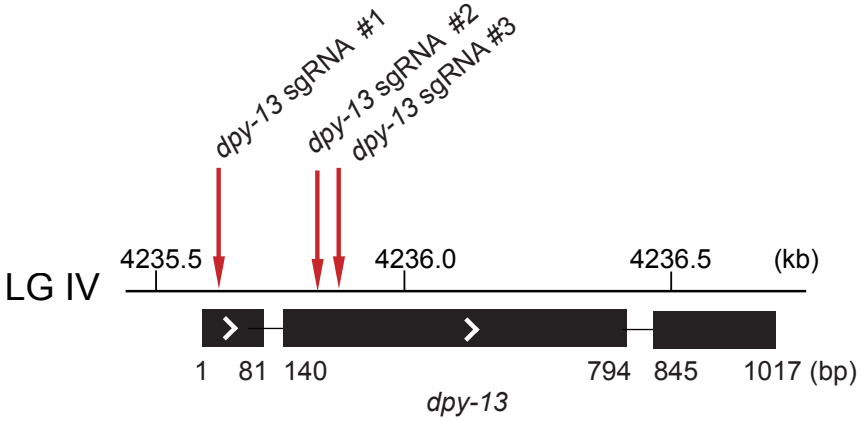

B

Expriment	sgRNA	Injected worm	F1s	Dumpy	Frequency
1	*dpy-13* sgRNA#1	40	324	1	0.3%
2	*dpy-13* sgRNA#2	35	24	3	12.5%
3	*dpy-13* sgRNA#3	35	20	0	0%

Figure S1. Positions of the sgRNAs-guided cleavage sites and summary of the microinjection experiments. (A) Schematic of the *dpy-13* gene. Positions of sgRNA-guided cleavage sites are indicated. (B) Summary of the microinjection experiments. The efficiency of the three sgRNAs targeting the *dpy-13* gene was assessed by scoring the dumpy phenotype. These results underestimated the percentage of cleavage events because some of the cleavage and repair events may not change the open reading frame and fail to elicit the visible dumpy phenotype.

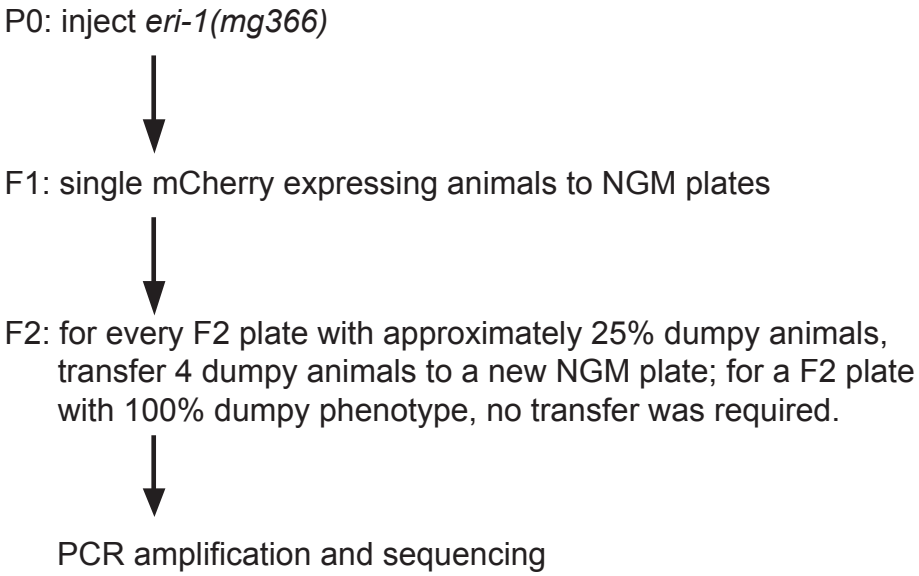

Figure S2. Schematic of the screen of CRISPR/Cas9-mediated chromosomal translocation. The ominant transformation marker mCherry was co-injected with the Cas9 and sgRNA expression plasmids. The F1 animals with mCherry expression were grown on NGM plates, and the phenotypes of the F2 progeny were examined. The dumpy animals were PCR amplified to detect chromosomal translocations and sequenced.

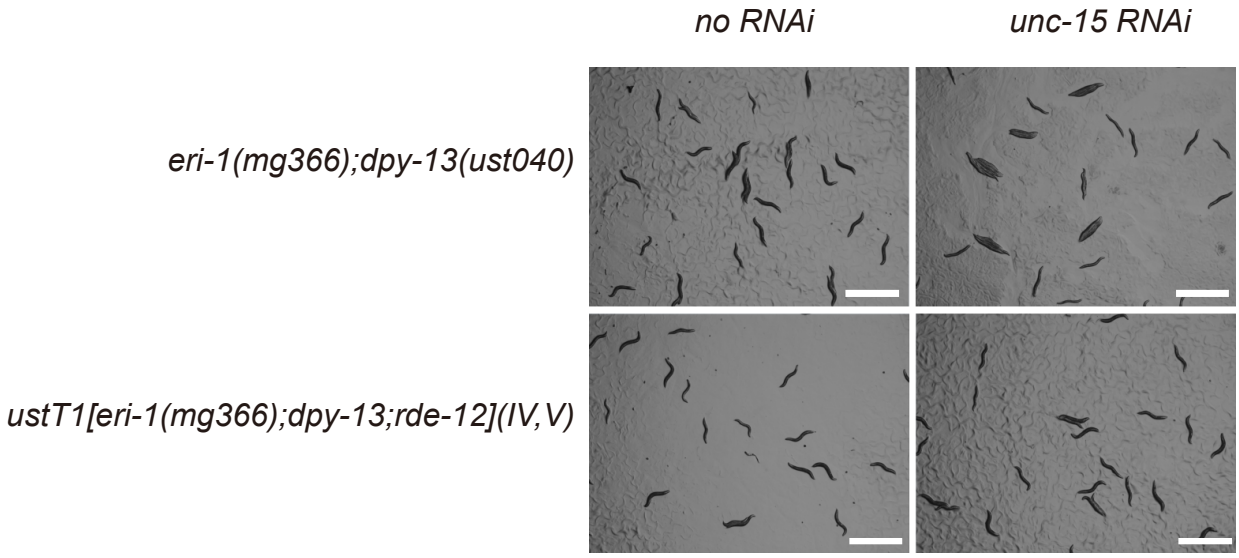

Figure S3. The chromosomal translocation strain *ustT1[eri-1(mg366);dpy-13;rde-12](IV,V)* suppresses exo-RNAi. Bleached embryos were grown on *unc-15* RNAi plates. Pictures were taken three days later. Scale bars, 1mm.

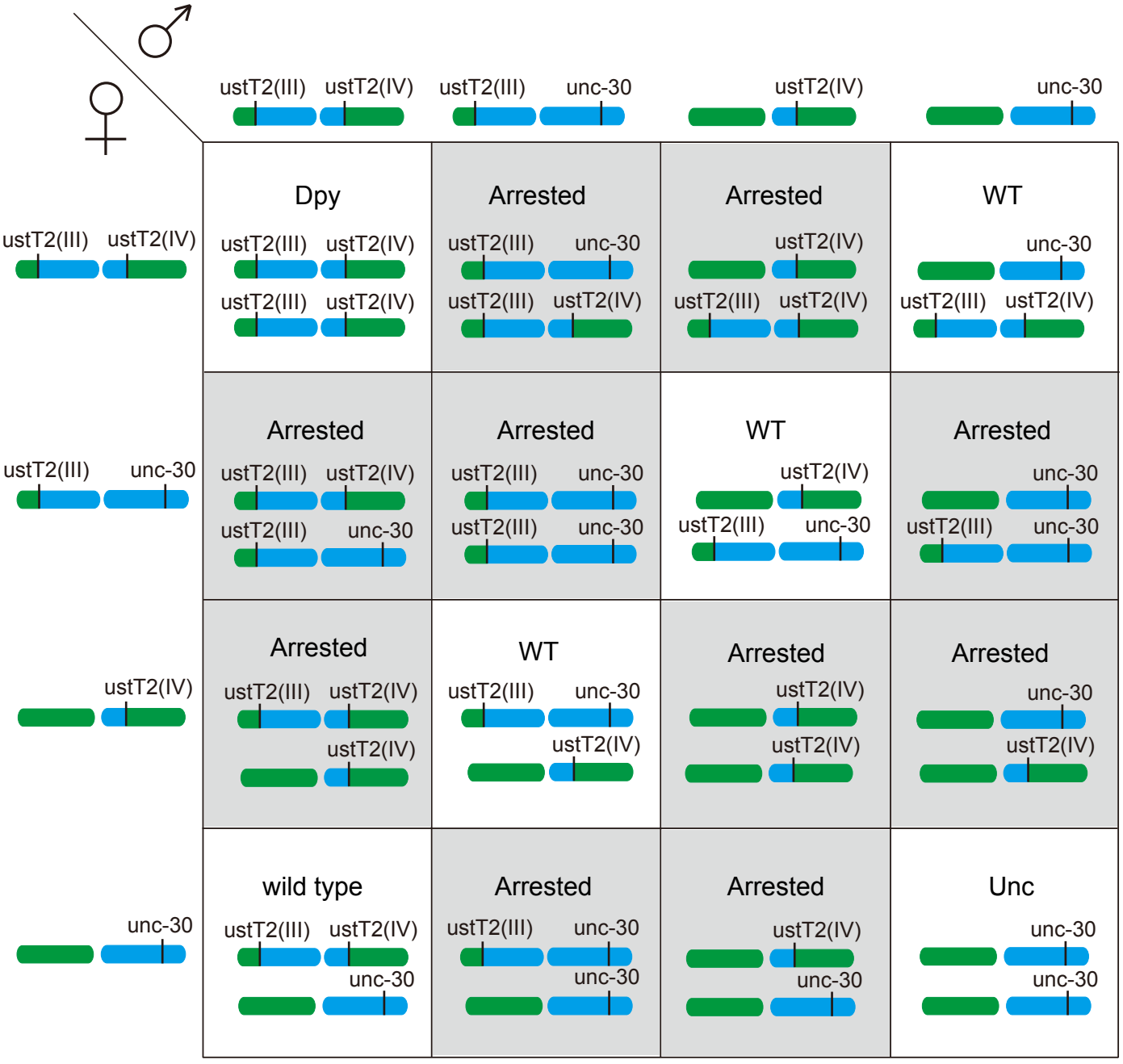
♂
♀
ustT2(III) ustT2(IV)
ustT2(III) unc-30
ustT2(IV)
unc-30
ustT2(III) ustT2(IV)
Dpy
ustT2(III) ustT2(IV)
ustT2(III) ustT2(IV)
Arrested
ustT2(III) unc-30
ustT2(III) ustT2(IV)
Arrested
ustT2(IV)
ustT2(III) ustT2(IV)
WT
unc-30
ustT2(III) ustT2(IV)
ustT2(III) unc-30
Arrested
ustT2(III) ustT2(IV)
ustT2(III) unc-30
Arrested
ustT2(III) unc-30
ustT2(III) unc-30
WT
ustT2(IV)
ustT2(III) unc-30
Arrested
unc-30
ustT2(III) unc-30
ustT2(IV)
Arrested
ustT2(III) ustT2(IV)
ustT2(IV)
WT
ustT2(III) unc-30
ustT2(IV)
Arrested
ustT2(IV)
ustT2(IV)
Arrested
unc-30
ustT2(IV)
wild type
ustT2(III) ustT2(IV)
unc-30
Arrested
ustT2(III) unc-30
unc-30
Arrested
ustT2(IV)
unc-30
Unc
unc-30
unc-30

Figure S4. Punnett square showing genotype and phenotype of the progeny that result from selfing a *unc-30(e191)/ustT2[ben-1;dpy-13](III,IV)* heterozygote. Phenotypes are indicated for each progeny class. Genotypes for gametes and zygotes are given by gene and rearrangement names and in drawings representing normal and translocation chromosomes with genetic markers. The normal LG III is shown as a green bar. The normal LG IV is shown as a blue bar, with a vertical line indicating the position of the *unc-30(e191)* allele. The translocation of *ustT2(III)* is shown as a green and blue bar with a vertical line indicating the position of the *ben-1* mutation caused by the translocation breakpoint on LG III. The translocation *ustT2(IV)* is shown as a green and blue bar with a vertical line indicating the position of the *dpy-13* mutation caused by the translocation breakpoint on LG IV. Unshaded boxes of the square represent viable progeny and shaded boxes represent aneuploid progeny, all of which are arrested during development. All wild-type progeny are heterozygous for the translocation chromosomes and the normal chromosomes. Dpy progeny are *ustT2(III,IV)* homozygotes, and Unc progeny are *unc-30* homozygotes. This figure is adapted from Edgley and Baillie (2006) (EDGLEY *et al.* 2006).

A

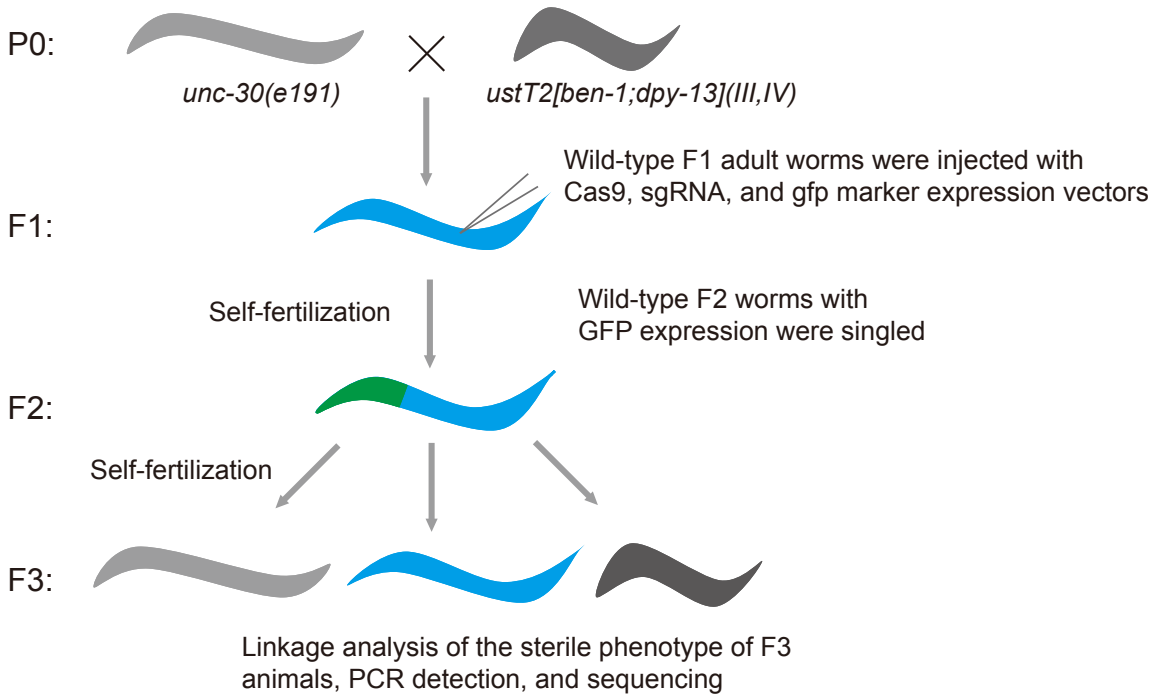

B

linkage type	sterile worms	chromosome carries the mutation
#1	F3 uncoordinated	normal chromosome
#2	F3 dumpy	translocated chromosome

Figure S5. Balancer construction of *csr-1* using the CRISPR/Cas9 system. (A) Schematic of the gene editing and balancer construction of the *csr-1* gene using the CRISPR/Cas9 technology. The dominant transformation marker mCherry was co-injected with the Cas9 and sgRNA expression plasmids. The sterile phenotype of F3 animals with different morphological markers was examined. (B) The linkage types between sterility and morphological phenotypes indicate the chromosomes on which the mutations are located.

A

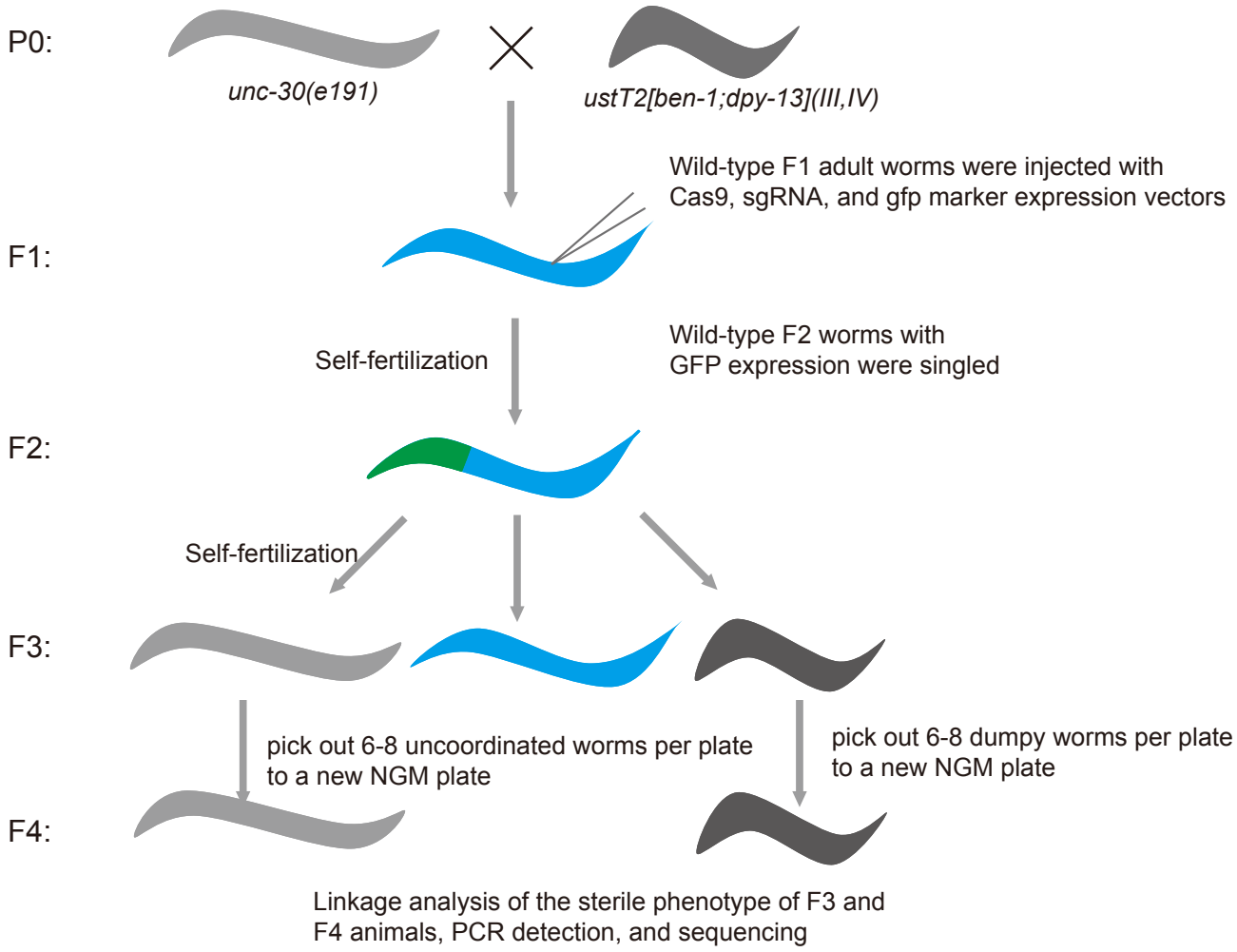

B

linkage type	sterile worms	chromosome carries the mutation
#1	F4 uncoordinated	normal chromosome
#2	F4 dumpy	translocated chromosome
#3	all F3 animals	both chromosomes

Figure S6. Genetic balancer generation of *mes-6*. (A) Schematic of the gene editing and balancer construction of the *mes-6* using the CRISPR/Cas9 technology. The dominant transformation marker mCherry was co-injected with the Cas9 and sgRNA expression plasmids. The sterile phenotype of F3 and F4 animals with different morphological markers was examined. (B) The linkage types between sterility and morphological phenotypes indicate the chromosomes on which the mutations are located.

Table S1. Summary of sgRNA sequences.

Name	Sequence
rde-12 sgRNA	GATTCTCGCGATAACCACGG(TGG)
dpy-13 sgRNA #1	GGACATTGACACTAAAATCA(AGG)
dpy-13 sgRNA #2	GTTATGAAGCTGACGGCGGA(CGG)
dpy-13 sgRNA #3	GGGCTTCGTTATGAAGCTGA(CGG)
ben-1 sgRNA	GAGTGATATCCGATGAGCAT(GGG)
csr-1 sgRNA #1	GACTTGCCCTGAACATCTTC(GGG)
csr-1 sgRNA #2	GATTCCATCTCGTTCCTCAG(CGG)
csr-1 sgRNA #3	GAAACCGTCATTCGTTCAGA(CGG)
mes-6 sgRNA #1	GATCGAAGTACAGAGGATTA(CGG)
mes-6 sgRNA #2	GAACAAGCGGTTGCAACTGT(CGG)
mes-6 sgRNA #3	GTTGTAACGGGTGGAACTTT(GGG)

Table S2. Summary of primer sequences for generation of sgRNA expression plasmids.

Name	Sequence
rde-12 sgRNA #2 F	GATTCTCGCGATAACCACGGGTTTTAGAGCTAGAAATAGC
rde-12 sgRNA #2 R	CCGTGGTTATCGCGAGAATCAAACATTTAGATTTGCAATT
dpy-13 sgRNA #1 F	GGACATTGACACTAAAATCAGTTTTAGAGCTAGAAATAGCAAGT
dpy-13 sgRNA #1 R	TGATTTTAGTGTCAATGTCCAAACATTTAGATTTGCAATTCAAT
dpy-13 sgRNA #2 F	GTTATGAAGCTGACGGCGGAGTTTTAGAGCTAGAAATAGCAAGT
dpy-13 sgRNA #2 R	TCCGCCGTCAGCTTCATAACAAACATTTAGATTTGCAATTCAAT
dpy-13 sgRNA #3 F	GGGCTTCGTTATGAAGCTGAGTTTTAGAGCTAGAAATAGCAAGT
dpy-13 sgRNA #3 R	TCAGCTTCATAACGAAGCCCAAACATTTAGATTTGCAATTCAAT
ben-1 sgRNA F	GTGTGATATCCGATGAGCATGTTTTAGAGCTAGAAATAGCAAGT
ben-1 sgRNA R	ATGCTCATCGGATATCACACAAACATTTAGATTTGCAATTCAAT
csr-1 sgRNA #1 F	GACTTGCCCTGAACATCTTCGTTTTAGAGCTAGAAATAGCAAGT
csr-1 sgRNA #1 R	GAAGATGTTCAGGGCAAGTCAAACATTTAGATTTGCAATTCAAT
csr-1 sgRNA #2 F	GATTCCATCTCGTTCCTCAGGTTTTAGAGCTAGAAATAGCAAGT
csr-1 sgRNA #2 R	CTGAGGAACGAGATGGAATCAAACATTTAGATTTGCAATTCAAT
csr-1 sgRNA #3 F	GAAACCGTCATTCGTTCAGAGTTTTAGAGCTAGAAATAGCAAGT
csr-1 sgRNA #3 R	TCTGAACGAATGACGGTTTCAAACATTTAGATTTGCAATTCAAT
mes-6 sgRNA #1 F	GATCGAAGTACAGAGGATTAGTTTTAGAGCTAGAAATAGCAAGT
mes-6 sgRNA #1 R	TAATCCTCTGTACTTCGATCAAACATTTAGATTTGCAATTCAAT
mes-6 sgRNA #2 F	GAACAAGCGGTTGCAACTGTGTTTTAGAGCTAGAAATAGCAAGT
mes-6 sgRNA #2 R	ACAGTTGCAACCGCTTGTTCAAACATTTAGATTTGCAATTCAAT
mes-6 sgRNA #3 F	GTTGTAACGGGTGGAACTTTGTTTTAGAGCTAGAAATAGCAAGT
mes-6 sgRNA #3 R	AAAGTTCCACCCGTTACAACAAACATTTAGATTTGCAATTCAAT

Table S3. PCR primer sequences to genotype strains with chromosome translocations.

Name	Sequence
dF (*dpy-13* primer F)	GATCAACGAAACAAGACTGTTGTA
dR (*dpy-13* primer R)	GATGAGGGATACGACGTATGC
rF (*rde-12* primer F)	GTTTTGTACAACAATGTTGCACC
rR (*rde-12* primer R)	GACGATCTGCCTCATCGAAG
bF (*ben-1* primer F)	CTCAAGATCGACGAGAACAG
bR (*ben-1* primer R)	ACTCATCAATCCATGACATGCC

Table S4. Primer sequences to genotype balancer strains with targeted mutations.

Name	Sequence
csr-1 primer F	GATCTCGCACCTGTGATTTTTC
csr-1 primer R	ACACTGTGATAGTGTTCGTAGC
mes-6 primer F	GTGCATGAGGTTATGCGCT
mes-6 primer R	GTGAAGAGCTTTGCACGCT

Table S5. Primer sequences for genotyping indels.

Name	Sequence
mg366 primer F	GATAAAACTTCGGAACATATGGGGC
mg366 primer R	ACTGATGGGTAAGGAATCGAAGACG
ok1644 primer F	CATTAACAGACGTCTGTAAACCTG
ok1644 primer R	CTTCCATAGGTGGTGTAACTGTC
gg098 primer F	AAAGAATTGCGCCCTAACCC
gg098 primer R	CATTGCCGATCTGTGTGGAG
ok2416 primer F	GACACACTGCTTGATGGGAC
ok2416 primer R	TATGCGGCAGTTTGCCGAT
ok3346 primer F	CGTGCCTTCTATTTGACTGTG
ok3346 primer R	CCCAAATCGCAACCATTTTTCA

File S1. Supporting References.

REFERENCE

Edgley, M. L., D. L. Baillie, D. L. Riddle and A. M. Rose, 2006 Genetic balancers. WormBook**:** 1-32.